

XII. LASER APPLICATIONS*

Academic Research Staff

Prof. S. Ezekiel

Graduate Students

R. E. Grove
L. A. Hackel
P. D. Henshaw

T. J. Ryan
J. R. Sneed

J. P. Sullivan
F. Y-F. Wu
D. G. Youmans

RESEARCH OBJECTIVES

Our interest is primarily in the application of lasers to a variety of measurement problems. In certain cases, the available lasers are not very suitable and considerable research has to be done to improve the laser performance. Several projects are in progress.

1. Laser Frequency Stabilization

The motivation for this work stems from the need for a long-term frequency stabilized laser in the precision measurement of length, i. e., length standards. Such a laser would find applications in earth-strain seismometry, in optical communication, and in fundamental measurements, in particular, those related to experimental relativity.

The task at present is to stabilize the frequency of the 5145 Å argon ion laser. The stabilization scheme employs, as an absolute frequency reference, a resonance absorption line, observed in a molecular beam of iodine. The absorption is measured by the resonance fluorescence induced by the laser in the molecular beam. Such an absorption line is an ideal reference element because of the isolated and unperturbed conditions in the beam. Moreover, since the molecular beam can be oriented at right angles to the laser beam, the width of the iodine resonance is limited to its natural width, which is inferred to be 100 kHz from lifetime measurements. Preliminary experiments indicate that it should be possible to stabilize the frequency of the laser to one part in 10^{13} . Thus far we have achieved a stability of 2 parts in 10^{11} .

2. High-Resolution Spectroscopy Using Molecular Beams

We are investigating the use of molecular beams for high-resolution spectroscopy. A single-frequency 5145 Å argon laser that can be tuned linearly over 0.05 Å is used to induce resonance fluorescence in a molecular beam of iodine. The resolution that we have achieved is less than 2×10^{-9} and is still limited by Doppler broadening attributable to molecular beam geometry. The laser, in the scanning mode, is capable of a resolution of better than 2×10^{-10} , as has been demonstrated with the use of a Fabry-Perot interferometer.

3. Single-Frequency cw Dye Laser

Continuous dye lasers offer the possibility of having a laser line of narrow spectral

*This work is supported by the U. S. Air Force - Office of Scientific Research (Contract F44620-71-C-0051) and by the Joint Services Electronics Programs (U. S. Army, U. S. Navy, U. S. Air Force) under Contract DAAB07-71-C-0300.

(XII. LASER APPLICATIONS)

width anywhere in the visible spectrum. This type of laser has many applications, such as spectroscopy and optical communication. The problem at present is that the dye laser frequency is not very stable and the tuning of the frequency is not continuous.

We propose to investigate the sources of laser frequency jitter in a cw dye laser so as to achieve a narrow spectral line width and, in addition, to develop continuous tuning schemes over limited ranges of approximately 1 Å.

This research will complement our work in high-resolution spectroscopy using molecular beams.

4. Pulsed Ion Laser Holography

The purpose of this research is to investigate possibilities for generating pulsed, high-power, multicolor laser output by using a mixture of noble gases, such as argon, krypton and xenon for interferometric and holographic applications.

For pulsed color holography we need a laser that puts out 3 primary colors of equal intensity simultaneously in one short pulse. The research involves the study of excitation mechanisms in the presence of a mixture of noble gases to yield the desired laser output.

Aside from color holography, a hologram that is recorded in 2 colors (or frequencies) and reconstructed with only one color displays contour lines (lines of equal distance from the hologram plate) superposed over the surface of the holographic image. The spacing between contour lines, which represents surface changes, is proportional to the frequency separation of the two colors used in the recording of the hologram.

We would like to use this surface contour generation method, which requires only a single short exposure, to study dynamic behavior of structures and materials and also to make growth measurement in biological subjects.

5. Flow Measurements

Laser Doppler techniques are being developed for measurement of both low-speed and high-speed fluid flow. A two-dimensional heterodyne scheme has been developed for velocity measurement in vortex rings and in the wake of a model helicopter rotor. For high-speed flow greater than 10^3 cm/s a scheme employing a Fabry-Perot cavity as a frequency discriminator is being investigated.

6. Closed-Loop Holographic Interferometry

We are exploring a new type of holographic interferometer. A diffuse object has been locked (within tens of angstroms) to its holographically stored virtual image by means of a servo loop. This technique is being applied in the detection of subfringe deformations of diffuse surfaces and in measurements of small changes in surface thickness.

S. Ezekiel

A. LASER MOLECULAR-BEAM TECHNIQUES FOR HIGH-RESOLUTION SPECTROSCOPY

USAF-OSR (Contract F44620-71-C-0051)

L. A. Hackel, D. G. Youmans, S. Ezekiel

A method employing a tunable single-frequency laser and a molecular beam has been used to obtain a high-resolution optical spectrum of the hyperfine structure of I_2 . In laser optical spectroscopy, the limiting factors are often Doppler and pressure broadening of the resonance lines. Saturated absorption has recently become a popular means of overcoming the Doppler effect.¹ The molecular-beam technique, however, offers control over Doppler broadening and also lacks the pressure broadening and pressure shift of the saturation techniques used for gas cells.

The experimental arrangement (Fig. XII-1) is similar to that used previously.² A single-frequency tunable 5145 Å argon ion laser excites the I_2 molecular beam. The induced fluorescence is detected by a photomultiplier. The excited transitions are the

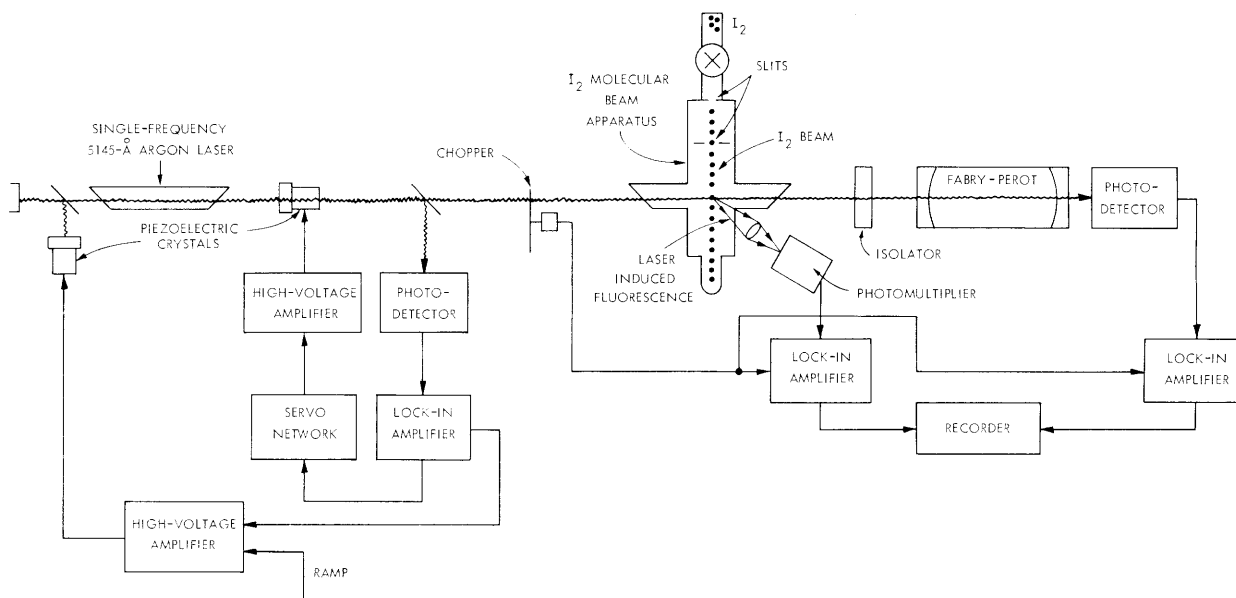


Fig. XII-1. Schematic view of the apparatus.

hyperfine components of the P(13) (43-0) and R(15) (43-0) lines between the $1^1\Sigma_g^+(X)$ and $3^1\Pi_{0u}^+(B)$ electronic states in I_2^{127} which fall within the bandwidth of the 5145 Å laser.³

Single-frequency operation is obtained by using a composite cavity made up of two cavities, one short and one long.⁴ A feedback loop with 1-kHz bandwidth maintains the coupling between the cavities. The laser frequency is scanned by changing the length of

(XII. LASER APPLICATIONS)

the short cavity by means of a piezoelectric crystal as shown in Fig. XII-1. In this locked mode of operation, the system linearity is determined by the linear response of the crystal and is not affected as much by the dispersion of the gain medium as it would be in an open-loop scan. Figure XII-2a shows a scan over a 1-MHz (FWMM) Fabry-Perot with a free spectral range of 300 MHz. The data indicate that laser short-term stability is better than 100 kHz.

The molecular beam apparatus, shown in Fig. XII-1, is a high-vacuum chamber into which I_2 molecules effuse through a narrow primary slit. A secondary slit, farther down, collimates the beam. The degree of collimation is determined by the width of the slits and the distance between them. The laser beam is chopped at 1 kHz. The I_2 fluorescence

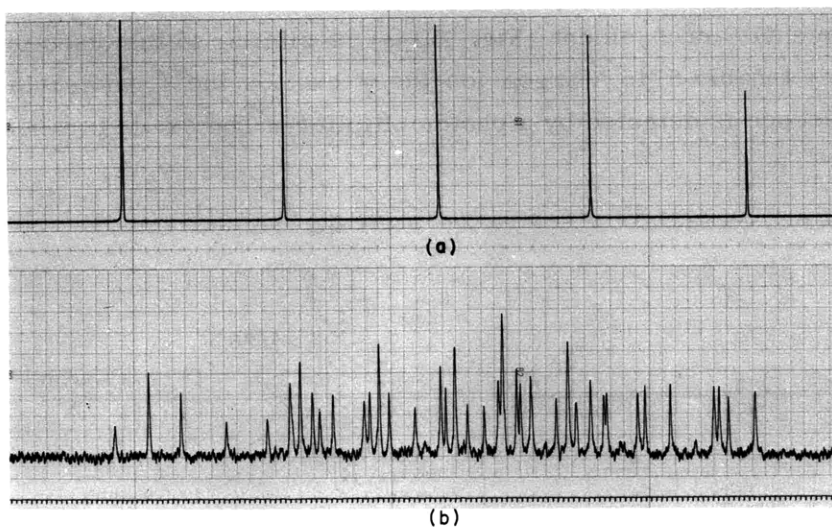


Fig. XII-2. Simultaneous recording as a function of laser frequency.
(a) Transmission resonances of the Fabry-Perot interferometer (free spectral range 300 MHz).
(b) Hyperfine structure of I_2 molecular beam ($\tau = 100$ ms).

incident on a photomultiplier is synchronously detected with a lock-in amplifier. The laser beam also excites the Fabry-Perot, and the fluorescence and Fabry-Perot data are recorded simultaneously.

The measured width of the lines shown in Fig. XII-2b is typically 3 MHz. The slit geometry dictated a Doppler width of 400 kHz. This contrasted sharply with lifetime measurements in the beam which indicated a natural width of 100 kHz.

In an effort to check on the possibility of small-angle collisions in the beam apparatus, the primary slit was reduced by a factor of four, thereby reducing both the number of molecules in the region between the slits and the possibility of collisions during the transit through the primary slit. At the same time the secondary slit was widened to

retain the same signal-to-noise ratio. In terms of slit geometry, the change resulted in an increase in beam angle from one to two milliradians. With the new slit geometry the resultant scan produced lines approximately 1.5 MHz wide. A portion of this spectrum is shown in Fig. XII-3. We shall try to observe the natural width of the I_2 transition. In

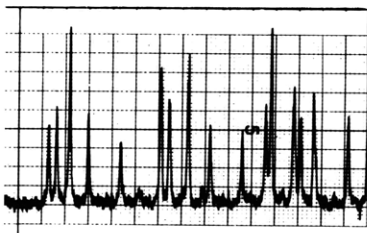


Fig. XII-3.
Portion of I_2 hyperfine structure showing lines approximately 1.5 MHz wide ($\tau = 30$ ms).

future experiments we shall employ narrower geometrical widths. The present resolution puts an 800-kHz upper limit on the natural linewidth.

When a more intense and geometrically broadened I_2 beam is used, other transitions, weaker than the prominent ones, are uncovered. Figure XII-4 shows the derivative of

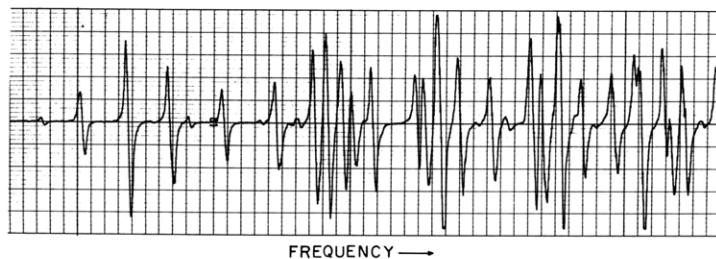


Fig. XII-4. Derivative of I_2 hyperfine structure showing existence of weaker lines not clearly observable in Fig. XII-2b ($\tau = 100$ ms).

I_2 transitions excited in this manner. The weak lines are shown dispersed among the stronger transitions associated with the P(13) and R(15) lines.

Laser molecular-beam techniques are clearly useful in high-resolution optical spectroscopy. Their application to laser frequency stabilization has already been demonstrated.⁵

References

1. P. H. Lee and M. S. Skolnick, *Appl. Phys. Letters* 10, 303 (1967); R. L. Barger and J. L. Hall, *Phys. Rev. Letters* 22, 4 (1969); M. S. Sorem and A. L. Schawlow, *Opt. Commun.* 5, 148 (1972).
2. S. Ezekiel and R. Weiss, *Phys. Rev. Letters* 20, 91 (1968).

(XII. LASER APPLICATIONS)

3. M. D. Levenson and A. L. Schawlow, Phys. Rev. A 6, 10 (1972).
4. P. W. Smith, IEEE J. Quant. Electronics, Vol. QE-1, No. 8, pp. 343-348, November 1965.
5. T. J. Ryan, D. G. Youmans, L. A. Hackel, and S. Ezekiel, Appl. Phys. Letters 21, 320 (1970).

B. MOLECULAR-BEAM STABILIZED ARGON LASER

USAF-OSR (Contract F44620-71-C-0051)

D. G. Youmans, L. A. Hackel, S. Ezekiel

We report the locking of the 5145 Å argon ion laser to an I_2 resonance observed in a molecular beam. A molecular beam external reference is attractive because transitions observed in the isolated conditions in the beam do not suffer frequency shifts caused by collisions or collisional broadening and, if the molecular beam is excited orthogonally by the laser, Doppler broadening can be virtually eliminated.

Resonance fluorescence induced in a molecular beam of iodine by a single-frequency 5145 Å argon ion laser has been reported previously.¹ The I_2^{127} excited transitions are the hyperfine components of the P(13) R(15) (43-0) lines between the $1\Sigma_g^+$ (X) and the $3\Pi_{0u}^+$ (B) electronic states falling within the Doppler width of the 5145 Å laser.²

The experimental arrangement used for frequency stabilization is shown in Fig. XII-5. A single-frequency tunable 5145 Å argon ion laser excites an I_2 molecular beam (A) at

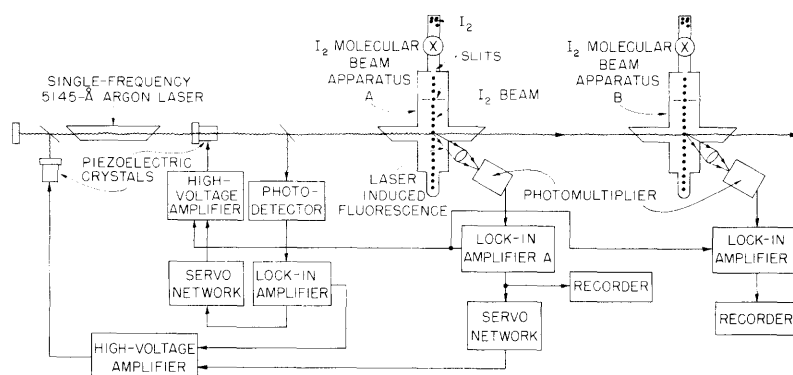


Fig. XII-5. Schematic view of the apparatus.

right angles. The laser-induced fluorescence is collected by a lens and focused onto a photomultiplier. Figure XII-6 shows the derivative of several of the I_2 lines excited by the laser as the laser is tuned across the gain curve. The derivative, which is used as

a frequency discriminant, is obtained by modulating the laser frequency and synchronously detecting the fluorescence signal in a lock-in amplifier. The laser frequency is locked to one of the I_2 transitions, e. g., the second one from the left (Fig. XII-6).

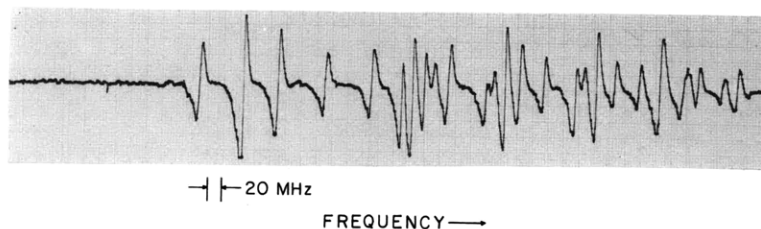


Fig. XII-6. Derivative of I_2 hyperfine structure observed in a molecular beam ($\tau = 30$ ms).

Measurement of laser frequency stability, at present, is done by monitoring the frequency discriminant associated with an identical I_2 transition that is excited by the stabilized laser in an independent molecular-beam apparatus (B) (Fig. XII-5).

Single-frequency laser operation is achieved by use of a composite cavity comprising two coupled cavities, one short and one long, a method similar to that of Smith.³ A feedback loop with a 1-kHz bandwidth maintains the coupling of the two cavities by locking the long cavity to the short cavity. The laser frequency may thus be scanned smoothly across the gain curve by linearly changing the length of the short cavity. This is accomplished by applying a ramp voltage to the piezoelectric crystal in the short cavity. The argon laser operates free from plasma oscillations. Techniques for suppressing plasma oscillations in our discharge-tube configuration have been reported previously.⁴

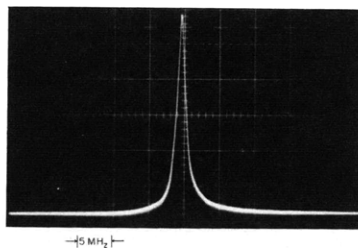


Fig. XII-7.

Output of 1-MHz Fabry-Perot when the laser is scanned at 4×10^{-5} s/MHz.

The short-term jitter of the laser frequency was investigated with a scanning Fabry-Perot (Tropel Model 216) that has an instrument width of 1 MHz and a free spectral range of 300 MHz. Figure XII-7 shows the output of the Fabry-Perot when the laser frequency is scanned at a rate of 4×10^{-5} s/MHz. The width of the Fabry-Perot resonance (Fig. XII-7) is identical with the instrument width and this puts an upper limit on laser

(XII. LASER APPLICATIONS)

jitter of less than 20 kHz. When the laser is scanned slowly over the Fabry-Perot resonance at the rate of 0.3 s/MHz the width is again 1 MHz, as shown in Fig. XII-8.

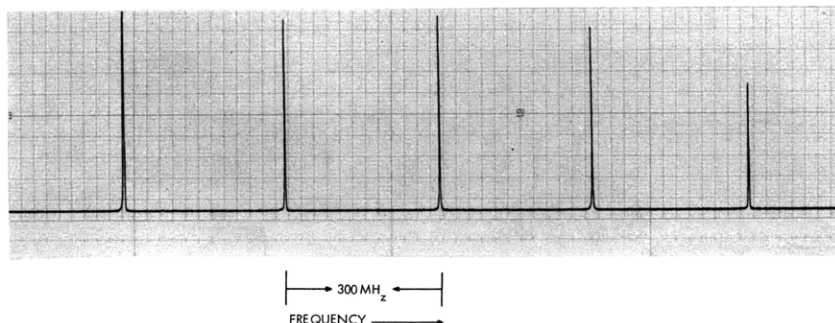


Fig. XII-8. Output of 1-MHz Fabry-Perot when the laser is scanned at 0.3 s/MHz.

The molecular-beam apparatus is a high-vacuum chamber into which I_2 molecules effuse through a narrow primary slit. The geometrical width of the I_2 beam is restricted by a secondary slit farther down the apparatus. The Doppler width of the I_2 transitions is then determined by slit geometry and is approximately 5 MHz in the experiments discussed here. (The natural width of the I_2 lines is of the order of 100 kHz inferred from lifetime measurements in the beam.¹) The laser-induced fluorescence is collected by a lens that is mounted external to the beam apparatus, and is then focused onto a photomultiplier with an S-20 photocathode.

To lock the laser to one of the I_2 lines, the output of lock-in amplifier A is fed into an integrator followed by a high-voltage amplifier that adjusts the length of the short cavity so as to maintain the laser frequency at the zero crossing of the discriminant; in other words, at the center of the selected I_2 line.

Figure XII-9 shows the outputs of the lock-in amplifiers associated with molecular beam A (trace a) and molecular beam B (trace c) when the laser is locked to one of the I_2 transitions observed in apparatus A. The output of lock-in amplifier B indicates that the laser frequency drift is less than 20 kHz (or $\Delta\nu/\nu < 3 \times 10^{-11}$) for the duration of the run which lasted approximately 20 min. The time constant in lock-in amplifier B at the beginning is 30 ms and is then changed to 1 second. A better and a more elegant measurement of frequency stability could be achieved by beating the output of two independently stabilized lasers. We shall do this soon, giving particular emphasis to frequency resetability.

The results of the preliminary stabilization scheme described here are very encouraging, even though much refinement is still needed. The argon laser is still the cause of many difficulties. Considerable work has been done to obtain adequate short-term laser frequency stability.

(XII. LASER APPLICATIONS)

The use of a molecular-beam reference promises a high degree of long-term stability and resetability of the laser frequency. The major drawback in this type of stabilization

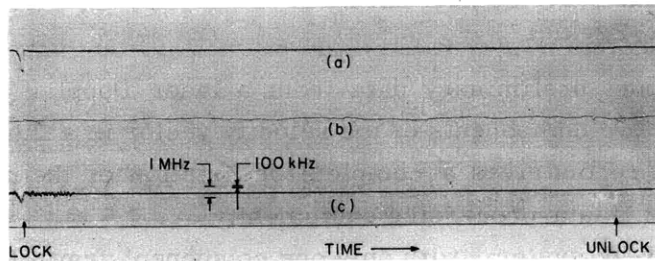


Fig. XII-9. Time recording of laser frequency drift.
(a) Output of lock-in amplifier A.
(b) Laser power.
(c) Output of lock-in amplifier B.
 $\tau = 30$ ms; later $\tau = 1$ s.
Total elapsed time = 20 min.

is the nonorthogonality between laser beam and molecular beam, which causes a Doppler shift. This Doppler shift, however, can be converted into a Doppler broadening by reflecting the laser beam back on itself through the molecular-beam apparatus. A more promising method for eliminating shifts caused by misalignment is to lock the laser to the saturated absorption dip at the center of the I_2 transition in the beam. It would certainly be interesting to find out how a molecular beam reference would eventually compare with a saturated absorption reference in a gas cell,⁵ especially with respect to long-term stability and resetability.

References

1. S. Ezekiel and R. Weiss, Phys. Rev. Letters 20, 91 (1968).
2. M. D. Levenson and A. L. Schawlow, Phys. Rev. A 6, 10 (1972).
3. P. W. Smith, IEEE J. Quant. Electronics, Vol. QE-1, p. 343, 1965.
4. D. C. Galehouse, U. Ingard, T. J. Ryan, and S. Ezekiel, Appl. Phys. Letters 18, 13 (1971).
5. R. L. Barger and J. L. Hall, Phys. Rev. Letters 22, 4 (1969); J. L. Hall and R. L. Barger, Proc. Twenty-third Annual Symposium on Frequency Control, U.S. Army Electronics Command, Fort Monmouth, New Jersey, 1969.

(XII. LASER APPLICATIONS)

C. TWO-DIMENSIONAL LASER DOPPLER VELOCIMETER

Joint Services Electronics Programs (Contract DAAB07-71-C-0300)

Partially supported by Naval Air Systems Command

J. P. Sullivan, S. Ezekiel

In a previous report preliminary data from a laser Doppler velocimeter (LDV) capable of measuring two components of the velocity vector in a fluid flow were presented.¹ The present report gives a complete description of the LDV system, with special emphasis on the data-processing equipment.

A diagram of the LDV system, with only one component drawn for clarity, is shown in Fig. XII-10. The LDV, which is a dual scatter system, described by Rudd² and by Lennert et al.,³ measures the Doppler shift of laser light scattered from particles in the flow field. The velocity of the particle, which is approximately the fluid velocity, is given by

$$V = \frac{f_D \lambda}{2 \sin \theta/2},$$

where V is the component of velocity in the plane of the two beams and perpendicular to the bisector of the angle between them, f_D is the frequency of the Doppler shift, λ is the laser wavelength, and θ is the angle between the two beams. In the present experiment the particles are oil particles, 2.0- μm in diameter, generated by a standard mist lubricator normally used to lubricate high-speed bearings.

As shown in Fig. XII-10, the laser beam is divided by a prism type of beam splitter with nonabsorbing beam-splitting interface. This method of dividing the laser beam is preferable to other systems in which mirrors and beam splitters are used, since only one standard optical component is needed and the path lengths (distance from laser to measuring point) of the two beams are equal.

A two-component system is constructed by adding a second beam splitter (rotated 90° with respect to the first) to form four parallel beams. The pattern of the four beams is shown in Fig. XII-11. The polarization of the beams is chosen to maximize the signal and to eliminate cross talk between the two dimensions. By placing an analyzing polaroid in front of the photomultiplier tube, either of the velocity components can be chosen with no interference from the other. This is possible because the polarization is changed only slightly by the scattering process. At present, both components are processed simultaneously through one photomultiplier tube, by using the electronic system described below. The two components could be processed separately by splitting the scattered radiation with a polarizing beam splitter and using two photomultiplier tubes and two sets of electronics equipment.

The electronic system for processing the LDV signal is one suggested by Iten⁴ for

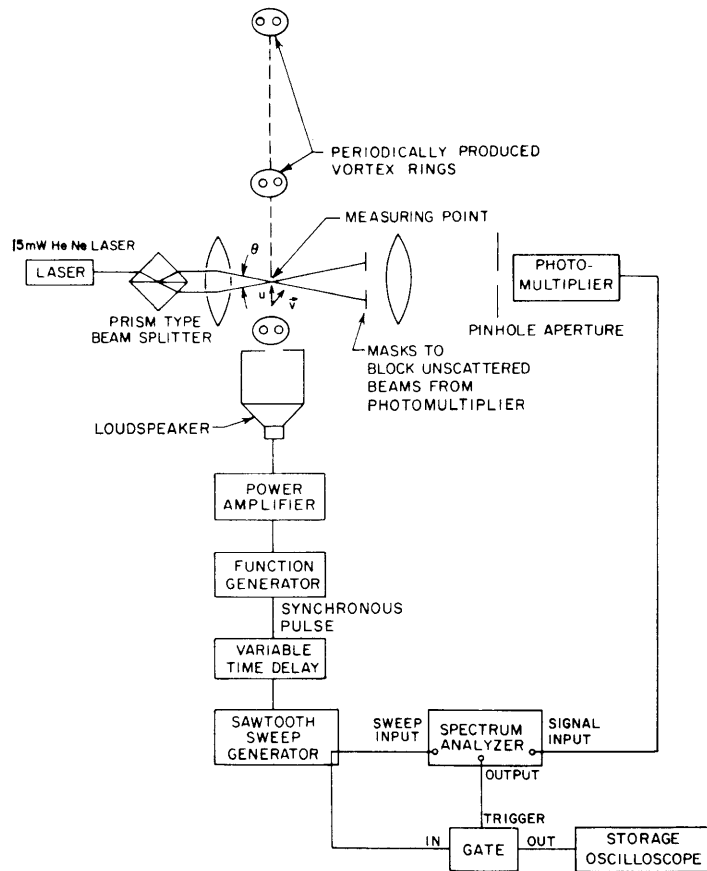


Fig. XII-10. One-dimensional LDV system.

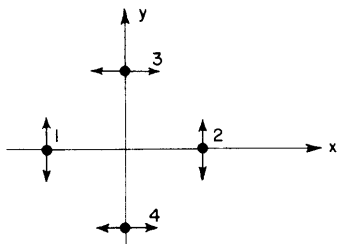


Fig. XII-11.

Beam pattern for two-dimensional LDV looking toward the laser. Arrows indicate the direction of polarization. Beams 1 and 2 measure the velocity component in the x direction, and beams 3 and 4 in the y direction.

(XII. LASER APPLICATIONS)

use with periodic flow fields. This "sampling" system for use with periodically produced vortex rings may be described in terms of the time diagrams shown in Fig. XII-12 and the equipment layout in Fig. XII-10. The function generator initiates a pulse that is amplified and used to drive a loudspeaker which forms a vortex ring at a sharp-edged orifice. A synchronous pulse is also taken off of the function generator (Fig. XII-12a).

Velocity vs time, as the vortex ring goes past the measuring point, is illustrated in Fig. XII-12b. This is proportional to frequency vs time of the output signal of the photomultiplier tube which is fed into the input of the spectrum analyzer. The synchronous pulse from the function generator initiates a time delay which starts the sawtooth sweep

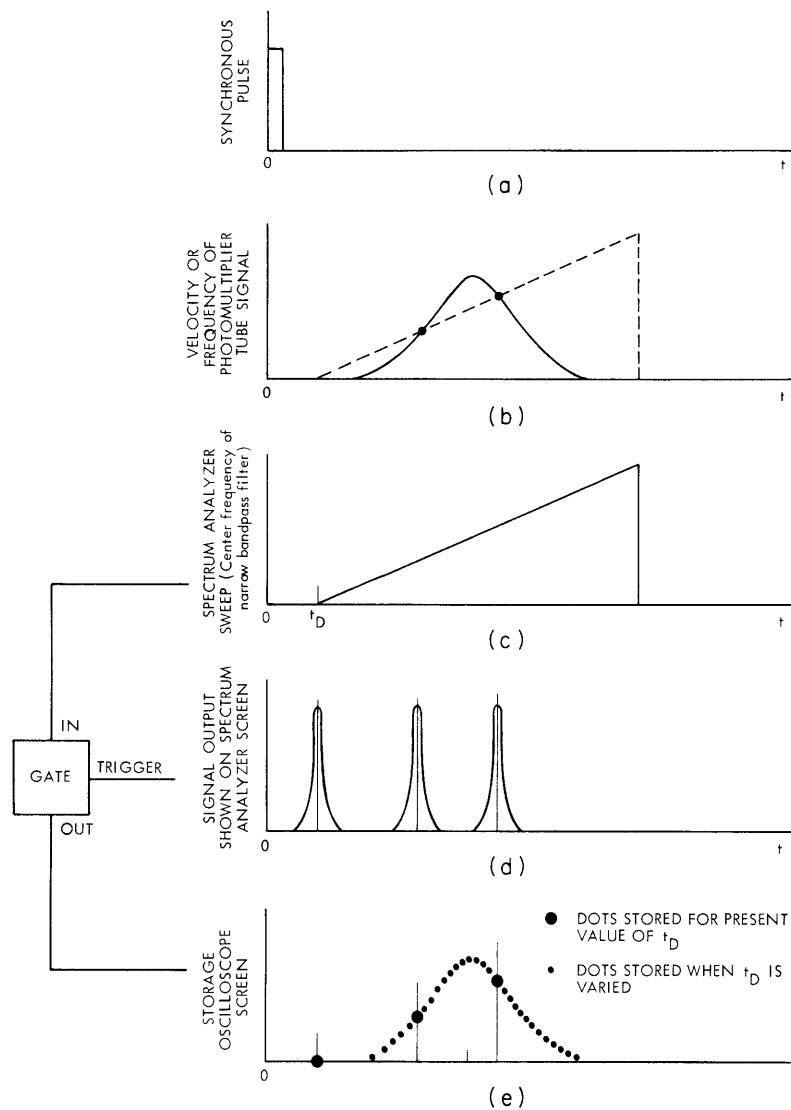


Fig. XII-12. Time diagrams for the electronic systems.

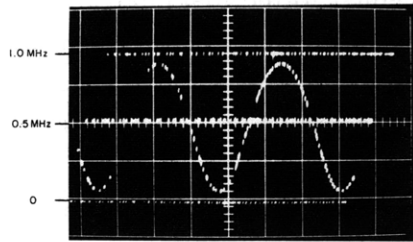


Fig. XII-13.

Demodulation of test signal.
 $f_o = 500 \text{ kHz}$
 $\Delta f = 450 \text{ kHz}$
 $f_M = 33 \text{ Hz}$
 Time scale = 10 MHz/cm.

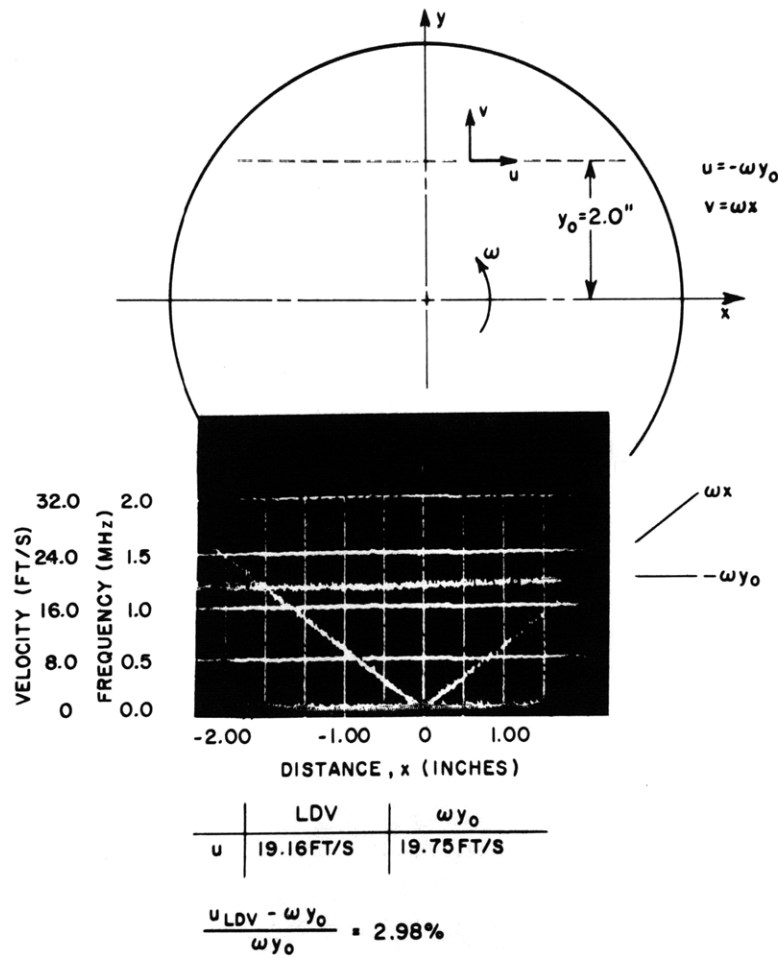


Fig. XII-14. Linearity and velocity check by using a spinning disk.

(XII. LASER APPLICATIONS)

generator (Fig. XII-12c) for the spectrum analyzer after a time t_D . The linear sawtooth represents the center frequency of the narrow filter of the spectrum analyzer. When the frequency from the photomultiplier tube is equal to the instantaneous frequency of the narrow bandpass filter of the spectrum analyzer a pip will occur on the spectrum analyzer face and at the spectrum analyzer output (Fig. XII-12d). This condition can be determined by superposing Fig. XII-12c on Fig. XII-12b. The linear sawtooth is fed to the input of a gate which is only opened when a pip occurs on the spectrum analyzer. The output of the gate (in this case, 3 spots, see Fig. XII-12e) is stored on a storage oscilloscope. The three spots correspond to a zero-frequency marker and 2 points on the velocity vs time curve which we wish to determine. By varying the time delay, the remaining points on the velocity curve can be stored.

The results of demodulating a test oscillator signal varying from 50 kHz to 950 kHz at a rate of 33 Hz are shown in Fig. XII-13.

The entire LDV system was checked by measuring two components of the velocity

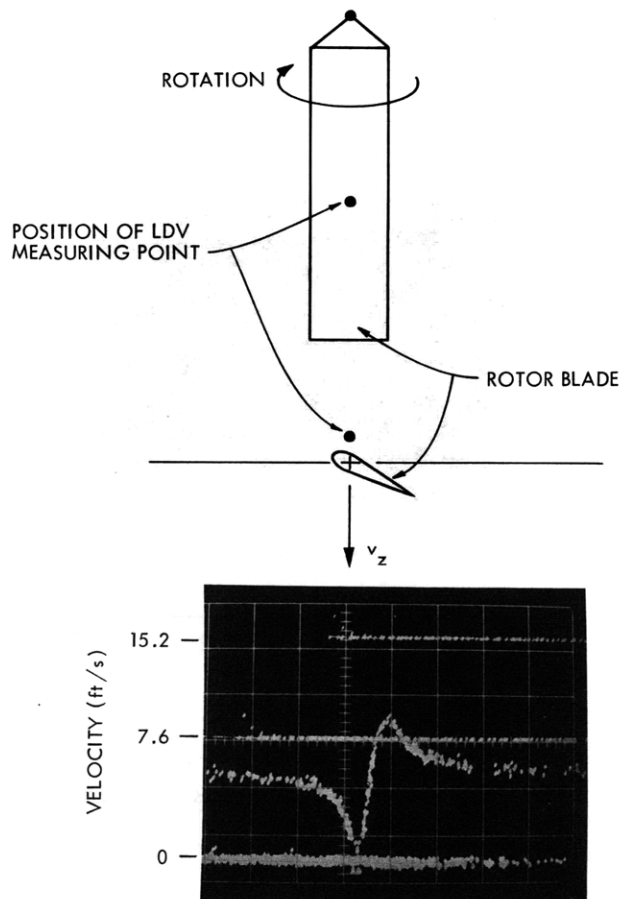


Fig. XII-15. Example of helicopter rotor data V_z component of velocity vs time at point shown in the sketch. Time scale = 2 MHz/cm.

of a spinning disk as the disk was traversed across the measuring point. The x component of velocity $U = -\omega y$ should be a constant and the y component $V = \omega x$ should vary linearly as the disk moves in the x direction. The results of this check, shown in Fig. XII-14, indicate that the linearity of the electronics system is excellent and that the velocity error is within experimental error in determining the rpm of the disk. The ambiguity in determining the direction of U and V is demonstrated in Fig. XII-14. The U component is always negative and the V component is negative for negative values of X.

The two-component LDV system has been used for extensive velocity measurements in periodically produced vortex rings and in the wake of a model helicopter rotor. Examples of the data from vortex rings were given in our previous report.¹

When the system is used for helicopter rotor measurements, the model rotor is placed in the position of the vortex ring generator shown in Fig. XII-10, and a synchronous signal from the rotating shaft is used to initiate the electronic data-processing system.

An example of data from the rotor measurements is shown in Fig. XII-15. The oscilloscope trace shows velocity vs time at a point half-way out and a little above the rotor blade. The experimental curve of the V_z component of velocity shows the classical signature of a lifting airfoil.

References

1. Quarterly Progress Report No. 104, Research Laboratory of Electronics, M. I. T., January 15, 1972, pp. 142-145.
2. M. J. Rudd, J. Phys. E 2, 55-58 (1969).
3. A. E. Lennert, E. B. Brayton, and F. L. Crossay, AEDC-TR-70-101, "Summary Report of the Development of a Laser Velocimeter to Be Used in Arnold Engineering Development Center Wind Tunnels," July 1970.
4. P. Iten, Private communication.

D. MULTIPLE-FREQUENCY HOLOGRAPHY USING PULSED ION LASERS

Joint Services Electronics Programs (Contract DAAB07-71-C-0300)

P. D. Henshaw, S. Ezekiel

The use of two-frequency holography to produce contour fringes on objects has been well documented,¹⁻⁶ but all schemes share a common difficulty in that the optics necessary to produce the proper reconstruction geometry limit the system. Careful alignment is necessary to avoid poor fringe localization or even complete destruction of the contours. We have developed a system in which alignment is not critical, fringe

(XII. LASER APPLICATIONS)

localization is guaranteed, and the contours may be viewed in white light. Because the object and reference beams travel nearly the same distance, lasers with limited coherence can be used to record the hologram. These advantages result from use of an extremely simple recording and reconstruction geometry, which is shown in Fig. XII-16.

Let (x_o, y_o, z_o) be an object point where the coordinates are defined relative to the center of the hologram plate. Similarly, let the reference source be located at (x_r, y_r, z_r) . In reconstruction, let the reconstructing source be at (x_c, y_c, z_c) , and the image point be at (x_i, y_i, z_i) . For convenience we prefer the reference and reconstruction

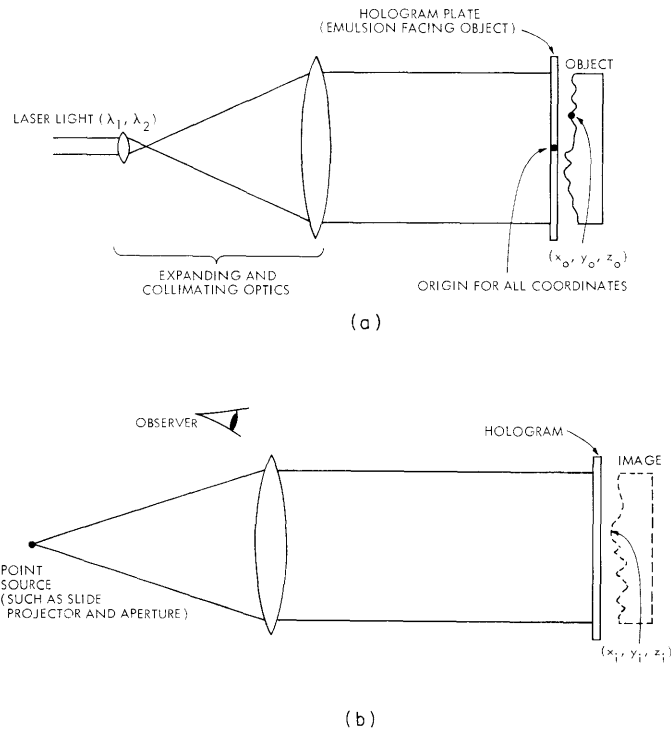


Fig. XII-16. (a) Recording and (b) reconstruction geometry.

beams to have the same coordinates for all colors if a multicolor laser is used.

It can be shown that the image location (x_i, y_i, z_i) is given by

$$\frac{1}{\lambda_c z_i} = \frac{1}{\lambda_r z_o} - \frac{1}{\lambda_r z_r} + \frac{1}{\lambda_c z_c} \quad (1)$$

$$\frac{x_i}{\lambda_c z_i} = \frac{x_o}{\lambda_r z_o} - \frac{x_r}{\lambda_r z_r} + \frac{x_c}{\lambda_c z_c} \quad (2)$$

$$\frac{y_i}{\lambda_c z_i} = \frac{y_o}{\lambda_r z_o} - \frac{y_r}{\lambda_r z_r} + \frac{y_c}{\lambda_c z_c} \quad (3)$$

By setting $z_r = z_c = \infty$ (using plane waves for reference and reconstruction), the magnification M_z in the z direction becomes

$$M_z \triangleq \frac{z_i}{z_o} = \frac{\lambda_r}{\lambda_c}, \quad (4)$$

which is equal to the ratio of the wavelengths used to record and reconstruct the hologram.

Equation 2 can be rewritten

$$x_i = x_o - \frac{z_o}{z_r} x_r + \frac{\lambda_r}{\lambda_c} \frac{z_o}{z_c} x_c. \quad (5)$$

If several holograms are recorded at different wavelengths, then as $z_o \rightarrow 0$, $x_i \rightarrow x_o$ and all images coincide in the x and y directions, independent of the reconstruction wavelength. This is exactly the requirement necessary for good contour fringes when using two wavelengths. Figure XII-16a shows the method that we use to meet the requirements. The depth contours are spaced at $\Delta z = \lambda^2 / 2\Delta\lambda$, independent of the reconstruction wavelength.⁴ This means that the fringes can be viewed in white light with no blurring of the contours. With the recording geometry shown in Fig. XII-16a we use a single beam to supply both reference and object beams. The hologram itself acts as the beam

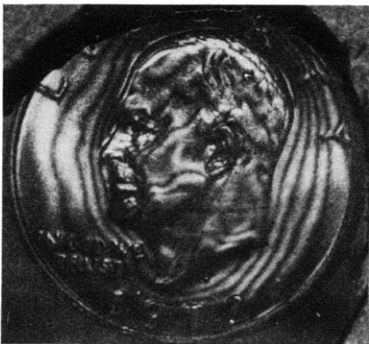


Fig. XII-17.

Hologram contour map of a silver dollar using 5353 Å and 5396 Å lines.

splitter, which means that only relative motion between the object and the hologram plate will affect the holographic recording. This is relatively easy to eliminate by fixing the plate to the object, thereby reducing the need for vibration isolation.

This recording geometry is ideal for pulsed holography, where the energy per pulse is limited. In conventional hologram arrangements with two beams used, much of the light scattered by the object is not collected by the hologram. In our case almost all of the light reaches the hologram.

Several contour maps of coins have been made using the 5353 Å and 5395 Å lines

(XII. LASER APPLICATIONS)

from a pulsed xenon laser. The fringe spacing is 34 μm . Figure XII-17 shows a reconstruction of a typical hologram in white light.

References

1. J. R. Varner, "Simplified Multiple-Frequency Holographic Contouring," Appl. Opt. 10, 212 (1971).
2. L. O. Heflinger and R. F. Wuerker, "Holographic Contouring via Multifrequency Lasers," Appl. Phys. Letters 15, 28 (1969).
3. W. Schmidt and A. F. Fercher, "Holographic Generation of Depth Contours Using a Flash-Lamp-Pumped Dye Laser," Opt. Commun. 3, 363-365 (1971).
4. B. P. Hildebrand and K. A. Haines, "Multiple-Wavelength and Multiple-Source Holography Applied to Contour Generation," J. Opt. Soc. Am. 57, 155 (1967).
5. J. S. Zelenka and J. R. Varner, "Multiple-Index Holographic Contouring," Appl. Opt. 8, 1431 (1969).
6. J. S. Zelenka and J. R. Varner, "A New Method for Generating Depth Contours Holographically," Appl. Opt. 7, 2107 (1968).

E. COHERENCE PROPERTIES OF A FLASH-LAMP-PUMPED DYE AMPLIFIER

Joint Services Electronics Programs (Contract DAAB07-71-C-0300)

P. D. Henshaw, S. Ezekiel

The study of high-power ion lasers for multicolor holography has led us to investigate the use of a dye cell pumped by a flash lamp as an amplifier. Our objective was to combine the high gain of a flash-lamp-pumped dye with the relatively long coherence length of a gas laser.

A pulsed xenon laser was used as the master oscillator. This laser appears to be a good choice because high-power lines are available throughout the visible spectrum.^{1,2} Other desirable characteristics are a short pulse, which is compatible with a flash-lamp-pumped dye cell, and relatively narrow Doppler broadening attributable to the large atomic weight of xenon.

A block diagram of our apparatus is shown in Fig. XII-18. The xenon laser was excited by a 2-mF capacitor charged to 5000 V. We found this gave laser pulses of approximately 500 W (all lines) with a 2- μs pulsewidth. Although higher powers could be produced, we found this combination of voltage and capacitor gave us the largest energy pulses for the pulsewidth that we desired.

A coaxial dye cell and flash lamp (Candela Corporation CL 100E) was used as the amplifier. The dye cell was 10 cm long and 1 cm in diameter. Dye solution was pumped through the cell at a rate fast enough to cool it, but not so fast that turbulence destroyed the wavefront of the xenon laser as it propagated through the cell.

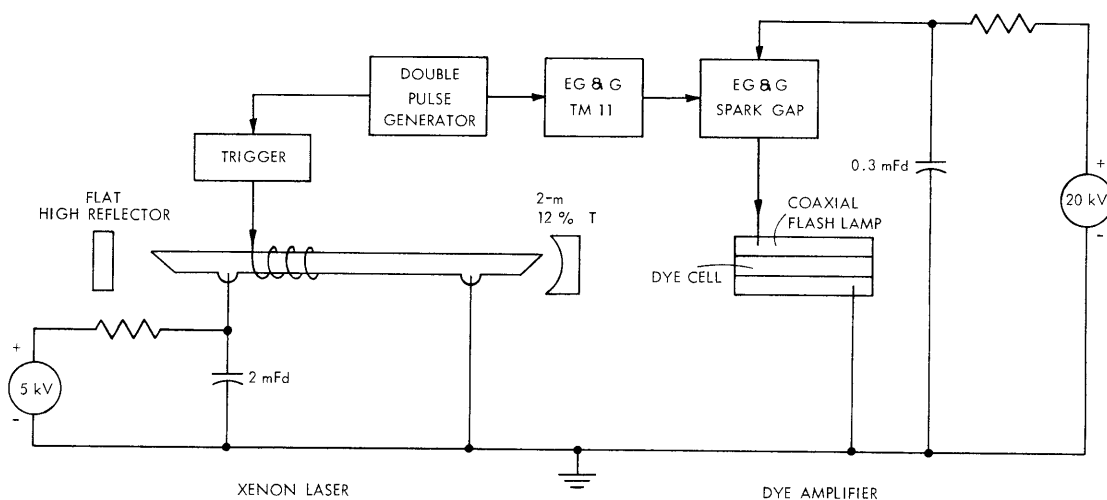


Fig. XII-18. Laser-amplifier arrangement.

Both the laser and the dye cell showed a consistent delay so that a double pulse generator had to be used to synchronize the pulses for maximum amplified energy.

The 5956 \AA line of xenon matched very well with rhodamine 6G, one of the most common and easily used dyes for lasers.³ The strongest line of xenon at 5353 \AA falls outside the bandwidth of rhodamine 6G. Fluorescein, another common dye, was used to amplify this wavelength.³ We were able to conduct experiments with both of these dyes to determine gain, coherence properties of the amplifier, and usefulness for holography. A single pass gain of 10 was obtained with rhodamine 6G and 3.6 with fluorescein.

Using a 10^{-4} molar solution of Na Fluorescein dye in water, we tested the ability of the dye amplifier to reproduce the input spectrum of the master oscillator by amplifying the 5265 \AA , 5353 \AA , and 5395 \AA lines of xenon. These lines were amplified by a factor of 3.6 for a flash-lamp energy of 60 J. The 5395 \AA and 5353 \AA lines were of the same peak power, while the 5265 \AA line was an order of magnitude smaller. The same gain was obtained for both separate and combined amplification of the three lines. This indicates that the dye behaves⁴ as an inhomogeneously broadened medium at a wavelength separation of 50 \AA . The results of this experiment indicate that we can produce a very high-power laser with two spectral lines separated 50 \AA . Such a laser would have applications in two-frequency contour generation.⁵

The spatial and temporal coherence of the xenon laser were preserved by the dye amplifier. Using a multimode xenon laser as the input, we measured the temporal coherence with a Michelson interferometer both before and after amplification. The fringe contrast was identical for all path-length differences. The measured coherence length was approximately 5 cm. The coherence properties of the dye amplifier were

(XII. LASER APPLICATIONS)

destroyed by heating the dye cell because of repeated pulsing. A 5-10 s delay between pulses was necessary to insure that this did not occur.

We have produced a reflection hologram of high quality, using a single pulse of amplified light at 5956 Å.

References

1. W. W. Simmons and R. S. Witte, "High Power Pulsed Xenon Ion Lasers," IEEE J. Quant. Electronics, Vol. QE-6, No. 7, pp. 466-469, July 1970.
2. J. P. Wheeler, "New Xenon Laser Line Observed," IEEE J. Quant. Electronics, Vol. QE-7, No. 8, p. 429, August 1971.
3. "Dye For Lasers," Kodak Publication No. JJ-169, Eastman Kodak Company, Rochester, New York, n. d.
4. H. S. Pilloff, "Simultaneous Two-Wavelength Selection in the N₂ Laser-Pumped Dye Laser," Appl. Phys. Letters 21, 339-340 (1972).
5. B. P. Hildebrand and K. A. Haines, "Multiple-Wavelength and Multiple-Source Holography Applied to Contour Generation," J. Opt. Soc. Am. 57, 155-162 (1967).